

Fast Solutions of Wideband RCS of Objects by Combing Improved Ultra-wide Band Characteristic Basis Function Method and Best Uniform Approximation

Wenyan Nie¹ and Zhonggen Wang²

¹School of Mechanical and Electrical Engineering
Huainan Normal University, Huainan, 232001, China
wynie5240@163.com

²School of Electrical and Information Engineering
Anhui University of Science and Technology, Huainan, 232001, China
zgwang@ahu.edu.cn

Abstract — The ultra-wide band characteristic basis function method (UCBFM) is an efficient approach to calculate wideband radar cross section (RCS) of objects, but its calculation errors at lower frequency points are great and the reduced matrix at each frequency point needs to be reconstructed, which are very time-consuming. To solve these problems, an effective numerical method for fast calculating wideband RCS of objects by combining improved UCBFM (IUCBFM) and best uniform approximation is proposed. This method improves the construction of the ultra-wide band characteristic basis functions (UCBFs) through solving the secondary level characteristic basis functions (SCBFs). In consideration of the mutual coupling effects among sub-blocks, the improved UCBFs contain more current information characteristics, which greatly improve the calculation precision at lower frequency points. Moreover, to avoid the reconstruction of reduced matrix at each frequency point, the best uniform approximation technology is used to fast predict the surface current at any frequency point in the given frequency band and further realize the fast calculation of wideband RCS of objects. Compared with traditional UCBFM, the method in this paper significantly improves the calculation accuracy and efficiency. Numerical results demonstrate that the proposed method is accurate and efficient.

Index Terms — Best uniform approximation, Method of Moments (MoM), Ultra-wide band Characteristic Basis Function Method (UCBFM), wideband radar cross section.

I. INTRODUCTION

Accurate prediction of wideband radar cross section (RCS) of objects is of great significance to the

studies of high-resolution radar imaging technology, anti-stealth and target identification. One of the most popular methods for radar cross sections (RCS) prediction is the frequency domain integral equation solved using method of moments (MoM) [1], but it places a heavy burden on memory and solving time when dealing with electrically large problems. Moreover, each frequency point in the given frequency band needs to be calculated one by one, it will be time-consuming. With the successive proposal of efficient methods, for example, fast multipole method (FMM) [2], multilevel fast multipole method (MLFMM) [3,4], adaptive integration method (AIM) [5], adaptive cross approximation (ACA) algorithm [6], and characteristic basis function method (CBFM) [7-9], the calculation efficiency by these methods at single frequency point is greatly improved. However, if the RCS is highly frequency dependent, one needs to do the calculations at finer increment of frequency to obtain an accurate representation of the frequency response, which must be computationally intensive. Thus, how to utilize the information carried by few frequency points to obtain wideband RCS in the given frequency band is of great importance. Therefore, scholars put forward many efficient methods. In [10], MLFMM is combined with impedance interpolation technology to analyze the wideband electromagnetic scattering problems. In [11], MLFMM is combined with the best uniform approximation to calculate the wideband RCS of objects. However, all the above methods still rely on an iteration method to solve linear equations, which needs to face unpredictable problems of convergence rate. In [12-14], asymptotic waveform evaluation (AWE) technology is used to analyze the wideband electromagnetic scattering problems and achieves good results. But this technology needed to store dense impedance matrix and

frequency derivative of impedance matrixes, which enlarged the memory requirement. So in [15], AWE based on the CBFM (AWE-CBFM), is proposed to analyze the wideband electromagnetic scattering problems. In [16], adaptive modified CBFM combined with model-based parameter estimation technology (AMCBFM-MBPE) is proposed to analyze the wideband and wide-angle electromagnetic scattering problems. Though the above two methods utilized CBFM to accelerate the solving speed of interpolation point and reduce memory consumption, these two methods need to recalculate the characteristic basis functions (CBFs) at each interpolation point. Hence, in [17], an ultra-wide band characteristic basis function method (UCBFM) is proposed to analyze the wideband electromagnetic scattering problems, without having the construction of CBFs for each frequency repeatedly. The CBFs constructed at the highest frequency point, termed ultra-wide band characteristic basis functions (UCBFs), entail the electromagnetic behavior at lower frequency range; thus, it follows that they can also be employed at lower frequency points without going through the time consuming step of constructing them again. However, the calculation errors of the RCS by UCBFM are great at lower frequency points; its universality is not strong. The lower accuracy at lower frequency points can be explained that the procedure are employed at lower frequency points using the discretization carried out at the highest frequency, this could lead to an increase of the condition number when calculating the impedance matrix [17]. Moreover, the corresponding reduced matrix at each frequency point still needs to be reconstructed, which is time-consuming.

In consideration of the calculation errors by UCBFM are great at lower frequency points and the reduced matrix at each frequency point shall be reconstructed. An improved ultra-wide characteristic basis function method (IUCBFM) is presented in this paper. This approach fully considers the mutual coupling effects among sub-blocks, the secondary level characteristic basis functions (SCBFs) are calculated after the primary characteristic basis function (PCBFs) are obtained. Because IUCBFM considers the mutual coupling effects among sub-blocks, improved UCBFs (IUCBFs) contain more current information characteristics and have a stronger universality. Thus, it could greatly improve the calculation accuracy at lower frequency points. Furthermore, to avoid the reconstruction of reduced matrix at each frequency point, IUCBFM is combined with the best uniform approximation technology to quickly predict the surface current at any frequency point within the frequency band and further realize the calculation of wideband RCS of objects. The numerical results indicate that compared with traditional UCBFM, the method in this

paper has significant improvements in calculation accuracy and efficiency.

II. THE UCBFM

The UCBFM firstly divides the object into M blocks. Refer to the literature [18], the optimized selection of the number of dividing blocks is $M \approx 0.9N^{1/3}$, where N is the total number of the RWG basis functions. Then, it establishes a model at the highest frequency point f_h . Multi-angle plane wave excitations are set to irradiate each block. Suppose N_θ and N_ϕ respectively represent the numbers of plane wave excitations in directions of θ and ϕ , in total $N_{\text{pws}} = 2N_\theta N_\phi$ (two polarization modes are considered), noted as $\mathbf{E}_{ih}^{N_{\text{pws}}}$. To obtain PCBFs of each block, one must solve the following system:

$$\mathbf{Z}_{ii}(f_h) \cdot \mathbf{J}_{ih}^{CBF} = \mathbf{E}_{ih}^{N_{\text{pws}}}, \quad (1)$$

where, \mathbf{Z}_{ii} is an $N_i \times N_i$ self-impedance matrix of block i , for $i = 1, 2, \dots, M$, N_i represents the number of the unknown numbers in block i ; $\mathbf{E}_{ih}^{N_{\text{pws}}}$ is an $N_i \times N_{\text{pws}}$ excitation matrix; and \mathbf{J}_{ih}^{CBF} is the PCBFs matrix of dimension $N_i \times N_{\text{pws}}$.

Typically, the number of plane waves we have used to generate the CBFs would exceed the number of degrees of freedom (DoFs) associated with the block, to eliminate the redundant information in \mathbf{J}_{ih}^{CBF} caused by overestimation, an orthogonalization procedure based on singular value decomposition (SVD) method is used to reduce the final number of CBFs, only those whose relative singular values above a certain threshold, for example, $1.0E-3$, are retained as UCBFs. Suppose there are K UCBFs for each block after SVD, where K is always smaller than N_{pws} . The surface current can be expressed as a liner combination of the UCBFs as follows:

$$\mathbf{J} = \sum_{m=1}^M \sum_{k=1}^K \alpha_m^k(f) \mathbf{J}_m^{CBF_k}, \quad (2)$$

where, $\mathbf{J}_m^{CBF_k}$ represents the k^{th} UCBFs of block m ; and $\alpha_m^k(f)$ represents the unknown weight coefficients. Galerkin method is used to convert the traditional MoM equation into a linear equation about coefficient matrix $\boldsymbol{\alpha}(f)$. We can get a $KM \times KM$ reduced matrix:

$$\mathbf{Z}^R(f) \cdot \boldsymbol{\alpha}(f) = \mathbf{V}^R(f), \quad (3)$$

where, $\mathbf{V}_i^R(f) = \mathbf{J}^T \cdot \mathbf{E}_i(f)$, for $i = 1, 2, 3, \dots, M$; and \mathbf{T} represents transposition. $\mathbf{Z}^R(f)$ represents the reduced impedance matrix of dimension $KM \times KM$. Its detailed calculation expression can be expressed as below:

$$\mathbf{Z}^R(f) = \mathbf{J}^T \cdot \mathbf{Z}_{ij}(f) \cdot \mathbf{J}, \quad (4)$$

where, $\mathbf{Z}_{ij}(f)$ represents the impedance matrix between blocks i and j at frequency f . Because the dimensionality of $\mathbf{Z}^R(f)$ is small, $\boldsymbol{\alpha}(f)$ can be obtained by directly solving Eq. (3). Then, $\boldsymbol{\alpha}(f)$ is substituted into Eq. (2). In this way, the surface current \mathbf{J} at any frequency f can be obtained. Though UCBFs can be reused at each frequency point, when f changes, the impedance matrix $\mathbf{Z}_{ij}(f)$ needs to be recalculated and $\mathbf{Z}^R(f)$ also needs to be reconstructed. It can be seen from Eq. (4) that numerous vector–matrix–vector products are present in the reduced matrix calculation process. Thus, it is not advisable to reconstruct the reduced matrix at each frequency point.

III. THE IUCBFM

To improve the calculation accuracy of UCBFM at lower frequency points, the construction of UCBFs is improved by considering the mutual coupling effects among sub-blocks. A model is established at the highest frequency point f_h in the given frequency band and the number of plane wave excitations is reduced. For each plane wave excitation, the SCBFs are calculated after the PCBFs are obtained. The PCBFs of block i can be solved by the following formula:

$$\mathbf{Z}_{ii} \mathbf{J}_i^p = \mathbf{E}_i, \quad (5)$$

where, \mathbf{E}_i represents the excitation vector of block i , for $i=1,2,3,\dots,M$; \mathbf{Z}_{ii} represents the self-impedance of block i , with dimensionality of $N_i \times N_i$. The PCBFs of block i can be obtained by directly solving Eq. (5). After the PCBFs of each block are solved, according to Foldy-Lax equation theory [19,20], the SCBFs on a block are calculated by replacing the incident field with the scattered fields due to the PCBFs on all blocks except from itself. By solving Eq. (6), we can obtain the first-order SCBFs. Similarly, higher-order SCBFs can be calculated. If the second-order SCBFs are calculated, these SCBFs can be calculated as:

$$\mathbf{Z}_{ii} \mathbf{J}_i^{S1} = - \sum_{j=1(j \neq i)}^M \mathbf{Z}_{ij} \mathbf{J}_j^p, \quad (6)$$

$$\mathbf{Z}_{ii} \mathbf{J}_i^{S2} = - \sum_{j=1(j \neq i)}^M \mathbf{Z}_{ij} \mathbf{J}_j^{S1}. \quad (7)$$

By solving Eq. (6) and Eq. (7), we can obtain all-order SCBFs. Let N_θ^{new} and N_ϕ^{new} respectively indicate the number of plane wave excitations in the θ and ϕ directions in the IUCBFM. After Eq. (5), Eq. (6) and Eq. (7) are solved, each block can obtain $6N_\theta^{new} N_\phi^{new}$ CBFs, including $2N_\theta^{new} N_\phi^{new} \mathbf{J}_i^p$, $2N_\theta^{new} N_\phi^{new} \mathbf{J}_i^{S1}$ and $2N_\theta^{new} N_\phi^{new} \mathbf{J}_i^{S2}$. To reduce the linear dependency

among these CBFs, we also need to use an SVD procedure. After the SVD procedure, the CBFs are retained as IUCBFs. The construction of IUCBFs fully considers the mutual coupling effects among sub-blocks, this not only enables IUCBFs to contain more current information characteristics but also greatly decreases the number of plane wave excitations, which improves the construction efficiency of IUCBFs.

IV. THE BEST UNIFORM APPROXIMATION

To avoid the reconstruction of reduced matrix at each frequency point, IUCBFM is combined with the best uniform approximation [21] to analyze the wideband electromagnetic scattering problems. After Chebyshev nodes in the given frequency band are solved, IUCBFM is applied to calculate the surface current at each Chebyshev node. There is no need to recalculate CBFs at each Chebyshev node, because the IUCBFs can be reused at each Chebyshev node. Finally, the best uniform approximation technology is used to fast predict the surface current at any frequency point in the frequency band and further realize the fast calculation of wideband RCS.

For a given frequency band $f \in [f_a, f_b]$, it corresponds to range of wave-number $k \in [k_a, k_b]$. The normalized transformation of k is given by:

$$\tilde{k} = \frac{2k - (k_a + k_b)}{k_b - k_a}, \quad (8)$$

According to Eq. (8), the range of \tilde{k} is easy to obtain as $[-1, 1]$. Then, the surface current $I(k)$ can be calculated by:

$$I(k) = I \left(\frac{\tilde{k}(k_b - k_a) + (k_a + k_b)}{2} \right), \quad (9)$$

and the Chebyshev approximation for $I(k)$ is given by:

$$I(k) = I \left(\frac{\tilde{k}(k_b - k_a) + (k_a + k_b)}{2} \right) \approx \sum_{l=0}^{n-1} c_l T_l(\tilde{k}) - \frac{c_0}{2}, \quad (10)$$

where, $c_l = \frac{2}{n} \sum_{i=1}^n I(k_i) T_l(\tilde{k}_i)$, $T_l(\tilde{k})$ is the Chebyshev polynomial.

The recursion formula about $T_l(\tilde{k})$ is concluded as:

$$\begin{cases} T_0(\tilde{k}) = 1 \\ T_1(\tilde{k}) = \tilde{k} \\ \dots \\ T_{l+1}(\tilde{k}) = 2\tilde{k}T_l(\tilde{k}) - T_{l-1}(\tilde{k}) \end{cases}, \quad (11)$$

$\tilde{k}_i (i=1, 2, \dots, n)$ denotes the Chebyshev node within the range of normalized wave-number and its expression is:

$$\tilde{k}_i = \cos\left(\frac{i-0.5}{n}\pi\right), \quad (12)$$

the corresponding wave-number $k_i \in [k_a, k_b]$ could be obtained by:

$$k_i = \frac{\tilde{k}_i(k_b - k_a) + (k_a + k_b)}{2}. \quad (13)$$

By solving Eq. (10), the surface current of the object at any frequency point in the whole wideband can be got and further fast calculation of wideband RCS can be realized.

V. NUMERICAL RESULTS

To verify the validity and accuracy of the proposed method, three test samples are presented. All simulations are completed on a personal computer with an Intel(R) Core(TM) i3-2120 CPU with 3.3 GHz (only one core is used) and 4 GB RAM. The threshold of the SVD is set to 10^{-3} , and all the objects are illuminated by a normally incident \hat{x} -polarized plane wave with the incident direction of $(\theta, \phi) = (0^\circ, 0^\circ)$.

First, we consider the scattering problem of a PEC sphere with radius of 0.3 m over a frequency range of 0.1 GHz to 1 GHz. The geometry is divided into 2346 triangular patches with an average length of $\lambda/10$ at 1 GHz. The object is divided into 8 blocks, and each block is extended by $\Delta = 0.15\lambda$ in all directions, thus resulting in 5250 unknowns. Referring to the literature [17], we construct the CBFs for the UCBFM, 20 plane wave excitations in directions of θ and ϕ are set, this approach results in a total of 800 CBFs. After SVD, 106 UCBFs (average value) are retained on each block; the construction time of UCBFs is 256s. In IUCBFM, 8 plane wave excitations in directions of θ and ϕ are set and the second-order SCBFs are calculated. This results in only 384 CBFs for each block, including 128 PCBFs, 128 first-order SCBFs and 128 second-order SCBFs. Although the SVD procedure is respectively used on PCBFs and all-order SCBFs. After SVD, the numbers of J^P , J^{S1} , and J^{S2} retained on each block are shown in Table 1. It can be seen that the second-order SCBFs J^{S2} have a strong linear correlation and have small influences on final current. Thus, the calculation of the first-order SCBFs is enough. With the decreasing number of incidence wave excitations and dimensionality of CBFs matrix, the construction time of IUCBFs is 171s, with a higher efficiency. The $\theta\theta$ polarization bistatic RCS calculated at 300 MHz by UCBFM and IUCBFM are shown in Fig. 1. It can be seen that the IUCBFs contain more current information characteristics and have higher accuracy at lower frequency points. The number of UCBFs and the accuracy of the two methods mainly depend on the threshold of the SVD.

The computational time and accuracy of the two methods at different threshold of the SVD are shown in Table 2. The relative error Err is defined as $(\|\mathbf{I} - \mathbf{I}_{\text{MOM}}\|_2 / \|\mathbf{I}_{\text{MOM}}\|_2) \times 100\%$, where \mathbf{I}_{MOM} is the current coefficient vector computed at the frequency of 300 MHz by the MoM, and \mathbf{I} is the current coefficient vector computed by the UCBFM or the IUCBFM. $\|\cdot\|_2$ denotes vector-2 norm. Through a comparison of Err versus the threshold of the SVD given in Table 2, we find that the IUCBFM can yield a satisfactory result with a small threshold, and the IUCBFM has a higher efficiency. In consideration of the CPU time and the number of the UCBFs, the threshold of SVD is selected as 10^{-3} . With a frequency step of 9 MHz, the wideband RCS obtained by using UCBFM and IUCBFM are shown in Fig. 2. It can be seen that the results at the lower frequency points calculated by IUCBFM are more accurate than those calculated by UCBFM.

Table 1: Number of CBFs retained on each block after the SVD of IUCBFM

CBFs	1	2	3	4	5	6	7	8
J^P	52	52	52	52	52	52	52	52
J^{S1}	47	47	47	47	47	47	47	47
J^{S2}	0	0	0	0	0	0	0	0

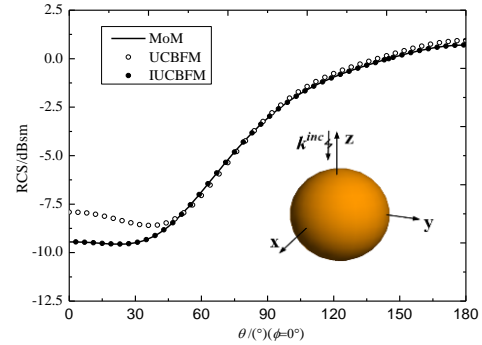


Fig. 1. Bistatic RCS in $\theta\theta$ polarization of the PEC sphere at 300 MHz.

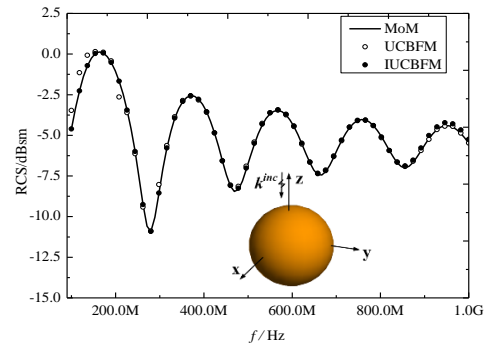


Fig. 2. Wideband RCS of the PEC sphere.

Table 2: CPU time and accuracy for varying the threshold

Threshold of SVD	UCBFM			
	SVD Time (s)	Number of UCBFs	CPU Time (s)	Relative Error (%)
0.05	129.6	337	208.1	15.23
0.01	129.7	510	236.9	11.23
0.005	129.9	638	248.5	9.13
0.001	130.1	852	289.3	7.78
0.0008	130.2	1053	302.3	7.70
0.0005	130.4	1261	335.1	7.68.
Threshold of SVD	IUCBFM			
	SVD Time (s)	Number of UCBFs	CPU Time (s)	Relative Error (%)
0.05	43.3	294	141.5	9.12
0.01	46.9	451	170.6	7.68
0.005	47.8	586	192.8	4.12
0.001	48.7	792	208.3	2.67
0.0008	48.8	905	225.4	2.63
0.0005	48.9	1026	254.6	2.60

We then consider the scattering problem of a complex conductor with top width of 0.15 m, bottom width of 0.075 m, height of 0.25 m. The frequency range starts from 0.1 GHz and terminates at 3 GHz. The discretization in triangular patches is conducted at 3 GHz with a mean edge length of $\lambda/10$, thus leading to 5084 unknowns. The target is divided into 4 blocks in the axis z direction. In UCBFM, 20 plane wave excitations in directions of θ and ϕ are set, 146 UCBFs are retained on each block. With a frequency step of 29 MHz, the wideband RCS of the target is calculated by UCBFM. When IUCBFM is used, 8 plane wave excitations in directions of θ and ϕ are set and the first-order SCBFs are calculated. 124 IUCBFs are retained on each block after SVD. The wideband RCS of the target is calculated by combing IUCBFM and the best uniform approximation (IUCBFM-Chebyshev). As shown in Fig. 3, the results obtained by the IUCBFM-Chebyshev with order of 10 agree well with the results obtained by the commercial software FEKO, which used the conventional MoM solver.

Finally, a 252.3744 mm PEC NASA almond is considered. We present the results for the problem of scattering over a frequency range from 0.1 GHz to 3 GHz. The geometry is divided into 2684 triangular patches with an average length of $\lambda/10$ at 3 GHz, thus resulting in 5752 unknowns. The target is divided into 4 blocks in the axis x direction. In UCBFM, 20 plane wave excitations in directions of θ and ϕ are set, 121 UCBFs are retained on each block. In IUCBFM, 8 plane wave excitations in directions of θ and ϕ are set. 102 IUCBFs are retained on each block. The wideband RCS calculated by using UCBFM and

IUCBFM-Chebyshev with order of 9 are shown in Fig. 4. It can be seen that the results calculated by IUCBFM-Chebyshev have a better coincidence with those of FEKO.

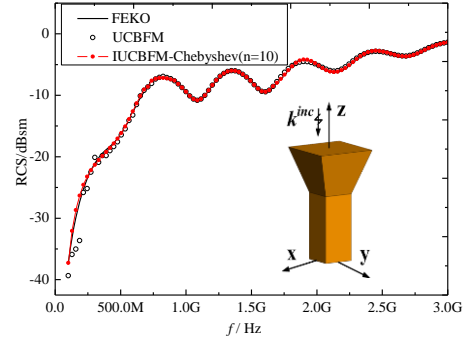


Fig. 3. Wideband RCS of the composite PEC conductor.

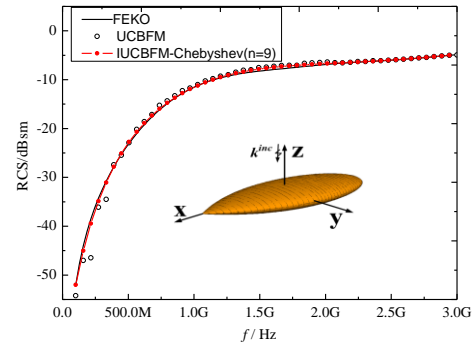


Fig. 4. Wideband RCS of the PEC NASA almond.

Table 3: CPU time and the relative error of the two methods

Problems	Method	UCBFs Construction (s)	Total Time (s)	Relative Error (%)
Problem 1: Sphere	MoM	---	52142	---
	UCBFM	256	39628	7.15
	IUCBFM	171	33469	2.95
Problem 2: Composite Conductor	FEKO	---	---	---
	UCBFM	268	31732	7.09
	IUCBFM-Chebyshev	206	4589	3.01
Problem 3: Nash Almond	FEKO	---	---	---
	UCBFM	297	26641	6.91
	IUCBFM-Chebyshev	198	3496	3.21

The CPU time and the relative error of the above three problems using UCBFM, IUCBFM and IUCBFM-Chebyshev are summarized in Table 3. We use the relative error (percent) of RCS to estimate the accuracy of the proposed method. The relative error is defined as:

$$\text{Rel.Error}(\%) = \left(\frac{1}{N} \sum_{k=1}^N \frac{|\text{RCS}_{f_k}^{\text{pm}} - \text{RCS}_{f_k}^{\text{ref}}|}{|\text{RCS}_{f_k}^{\text{ref}}|} \right) \times 100, \quad (14)$$

where $\text{RCS}_{f_k}^{\text{pm}}$ is the RCS provided by the UCBFM, or the IUCBFM at the frequency of f_k , $\text{RCS}_{f_k}^{\text{ref}}$ is the RCS provided by the MoM (FEKO), N is the total number of frequency points. Compared with the traditional UCBFM, IUCBFM improves the construction efficiency of UCBFs, but the calculation time of the wideband RCS does not decrease significantly. The reason for this is that the impedance matrix $\mathbf{Z}_{ij}(f)$ should be recalculated when the f changes, and the reduced matrix at each frequency point needs to be reconstructed, there are many vector–matrix–vector products in the calculation of the reduced matrix, so the computation cost of IUCBFM is very expensive. In order to avoid the reconstruction of reduced matrix at each frequency, the IUCBFM combined with the best uniform approximation is used to calculate the wideband RCS of problem 2 and problem 3. It can be seen from the calculation time of problem 2 and problem 3 that, because the reduced matrix reconstruction at each frequency point is cut down, the calculation efficiency of IUCBFM-Chebyshev is greatly improved.

VI. CONCLUSION

This paper puts forward an effective numerical method for calculating wideband RCS of objects by combining IUCBFM and best uniform approximation. This method improves the construction of UCBFs, the IUCBFs contain more current information characteristics and have a stronger universality, it improves the calculation accuracy at lower frequency points. In addition, in order to avoid the reconstruction of reduced matrix at each frequency point, the best uniform approximation technology is used to fast predict the surface current at any frequency point in the given frequency band and further realize the fast calculation of wideband RCS of objects. Several numerical results have indicated that compared with traditional UCBFM, the method proposed in this paper owns higher accuracy and efficiency.

ACKNOWLEDGMENT

This work was supported by the National Natural Science Foundation of China under Grant No. 61401003, the Natural Science Foundation of Anhui Provincial Education Department under Grant No. KJ2016A669, and the Natural Science Foundation of Huainan Normal University under Grant No. 2015xj09zd.

REFERENCES

[1] R. F. Harrington, *Field Computation by Moment*

- Method*. New York: Macmillan, pp. 22-57, 1968.
- [2] R. Coifman, V. Rokhlin, and S. Wandzura, "The fast multipole method for the wave equation: A pedestrian prescription," *IEEE Ant. Propag. Mag.*, vol. 53, no. 3, pp. 7-12, 1993.
- [3] J. M. Song, C. C. Lu, and W. C. Chew, "Multilevel fast multipole algorithm for electromagnetic scattering by large complex objects," *IEEE Trans. Antennas Propag.*, vol. 45, no. 10, pp. 1488-1493, 1997.
- [4] M. Chen, R. S. Chen, and X. Q. Hu, "Augmented MLFMM for analysis of scattering from PEC object with fine structures," *Applied Computational Electromagnetics Society (ACES) Journal*, vol. 26, no. 5, pp. 418-428, 2011.
- [5] E. Bleszynski, M. Bleszynski, and T. Jaroszewicz, "Adaptive integral method for solving large-scale electromagnetic scattering and radiation problems," *Radio Sci.*, vol. 31, no. 5, pp. 1225-1251, 1996.
- [6] Z. Liu, R. Chen, J. Chen, and Z. Fan, "Using adaptive cross approximation for efficient calculation of monostatic scattering with multiple incident angles," *Applied Computational Electromagnetics Society (ACES) Journal*, vol. 26, no. 4, pp. 325-333, 2011.
- [7] V. V. S Prakash and R. Mittra, "Characteristic basis function method: A new technique for efficient solution of method of moments matrix equations," *Microw. Opt. Technol. Lett.*, vol. 36, no. 2, pp. 95-100, 2003.
- [8] E. Lucente, A. Monorchio, and R. Mittra, "An iteration free MoM approach based on excitation independent characteristic basis functions for solving large multiscale electromagnetic scattering problems," *IEEE Trans. Antennas Propag.*, vol. 56, no. 4, pp. 999-1007, 2008.
- [9] K. Konno and Q. Chen, "The numerical analysis of an antenna near a dielectric object using the higher-order characteristic basis function method combined with a volume integral equation," *IEICE Trans. Commun.*, vol. E97-B, no. 10, pp. 2066-2073, 2014.
- [10] Z. H. Fan, Z. W. Liu, and D. Z. Ding, "Preconditioning matrix interpolation technique for fast analysis of scattering over broad frequency band," *IEEE Trans. Antennas Propag.*, vol. 58, no. 7, pp. 2484-2487, 2010.
- [11] T. Chao, Y. J. Xie, and Y. Y. Wang, "Fast solutions of wide-band RCS pattern of objects using MLFM with the best uniform approximation," *Journal of Electronics & Information Technology*, vol. 31, no. 11, pp. 2772-2775, 2009.
- [12] C. J. Reddy, M. D. Deshpande, and C. R. Cockrell, "Fast RCS computation over a frequency band using method of moments in conjunction with asymptotic evaluation technique," *IEEE*

- Trans. Antennas Propag.*, vol. 46, no. 8, pp. 1229-1233, 1998.
- [13] X. Wang, S. X. Gong, and J. L. Guo, "Fast and accurate wide-band analysis of antennas mounted on conducting platform using AIM and asymptotic waveform evaluation technique," *IEEE Trans. Antennas Propag.*, vol. 59, no. 12, pp. 4624-4633, 2011.
- [14] C. J. Reddy, M. D. Deshpande, and C. R. Cockrell, "Fast RCS computation over a frequency band using method of moments in conjunction with asymptotic waveform evaluation technique," *IEEE Trans. Antennas Propag.*, vol. 46, no. 8, pp. 1229-1233, 1998.
- [15] Y. F. Sun, Y. Du, and Y. Sao, "Fast computation of wideband RCS using characteristic basis function method and asymptotic waveform evaluation technique," *Journal of Electronics (in Chinese)*, vol. 27, no. 4, pp. 463-467, 2010.
- [16] G. D. Han, Y. H. Pan, and B. F. He, "Fast analysis for 3D wide-band & wide-angle electromagnetic scattering characteristic by AMCBFM-MBPE," *Journal of Microwaves*, vol. 25, no. 6, pp. 32-37, 2009.
- [17] M. Degiorgi, G. Tiberi, and A. Monorchio, "Solution of wide band scattering problems using the characteristic basis function method," *IET Microwaves Antennas and Propagation*, vol. 6, no. 1, pp. 60-66, 2012.
- [18] K. Konno, Q. Chen, K. Sawaya, and T. Sezai, "Optimization of block size for CBFM in MoM," *IEEE Trans. Antennas Propag.*, vol. 60, no. 10, pp. 4719-4724, 2012.
- [19] L. Tsang, C. E. Mandt, and D. H. Ding, "Monte Carlo simulations of the extinction rate of dense media with randomly distributed dielectric spheres based on solution of Maxwell's equations," *Optics Letters*, vol. 17, no. 5, pp. 314-316, 1992.
- [20] Z. G. Wang, Y. F. Sun, and G. H. Wang, "Analysis of electromagnetic scattering from perfect electric conducting targets using improved characteristic basis function method and fast dipole method," *J. Electromagn. Waves Appl.*, vol. 28, no. 7, pp. 893-902, 2014.
- [21] H. D. Raedt, K. Michielsen, and J. S. Kole, "Solving the Maxwell equations by the Chebyshev method: A one step finite-difference time-domain algorithm," *IEEE Trans. Antennas Propag.*, vol. 51, no. 11, pp. 3155-3160, 2003.



include computational electromagnetic methods, antenna theory and design.



Zhonggen Wang was born in Jiangsu Province, China, in 1981. He received the Ph.D. degree in Electromagnetic Field and Microwave Technique from the Anhui University of China, Hefei, P. R. China, in 2014. His current research interests include computational electromagnetics, signal and information processing techniques in electromagnetics.